The critical particle size for enhancing thermal conductivity in metal nanoparticle-polymer composites

Zexi Lu, Yan Wang, and Xiulin Ruan

Citation: Journal of Applied Physics **123**, 074302 (2018);
View online: https://doi.org/10.1063/1.5014987
View Table of Contents: http://aip.scitation.org/toc/jap/123/7
Published by the American Institute of Physics

The critical particle size for enhancing thermal conductivity in metal nanoparticle-polymer composites

Zexi Lu,[1] Yan Wang,[2] and Xiulin Ruan[1,a)]
[1]*School of Mechanical Engineering and the Birck Nanotechnology Center, Purdue University, West Lafayette, Indiana 47907, USA*
[2]*Department of Mechanical Engineering, University of Nevada, Reno, Reno, Nevada 89557, USA*

(Received 14 November 2017; accepted 26 January 2018; published online 16 February 2018)

Polymers used as thermal interface materials are often filled with high-thermal conductivity particles to enhance the thermal performance. Here, we have combined molecular dynamics and the two-temperature model in 1D to investigate the impact of the metal filler size on the overall thermal conductivity. A critical particle size has been identified above which thermal conductivity enhancement can be achieved, caused by the interplay between high particle thermal conductivity and the added electron-phonon and phonon-phonon thermal boundary resistance brought by the particle fillers. Calculations on the SAM/Au/SAM (self-assembly-monolayer) system show a critical thickness L_c of around 10.8 nm. Based on the results, we define an effective thermal conductivity and propose a new thermal circuit analysis approach for the sandwiched metal layer that can intuitively explain simulation and experimental data. The results show that when the metal layer thickness decreases to be much smaller than the electron-phonon cooling length (or as the "thin limit"), the effective thermal conductivity is just the phonon portion, and electrons do not participate in thermal transport. As the thickness increases to the "thick limit," the effective thermal conductivity recovers the metal bulk value. Several factors that could affect L_c are discussed, and it is discovered that the thermal conductivity, thermal boundary resistance, and the electron-phonon coupling factor are all important in controlling L_c. *Published by AIP Publishing.* https://doi.org/10.1063/1.5014987

I. INTRODUCTION

Nanocomposite materials are widely used nowadays due to their outstanding properties which cannot be achieved by single-phase materials. They can be implemented in conditions where a high thermal conductivity is desired for heat dissipation, or where a low thermal conductivity is desired for a large thermoelectric figure of merit ZT.[1–4] Besides, they play important roles in constructing controllable nanostructures, such as nanowires, nanotubes, and nanoparticles.[5] Many practical applications require us to optimize conflicting properties of materials to meet the demands. This could often be achieved by combining materials of different properties or adding one to another. Thus, predicting the property of the composites and understanding the physics and mechanism become important. More than one hundred years ago, Maxwell already presented a theoretical method for calculating the effective properties of particulate composites.[6] His pioneer work has served as a basis for many following studies through these years.

There have been a series of theoretical studies on the effective properties of composite materials. The effective medium approximation (EMA) has been most widely applied.[7–10] Hasselman and Johnson developed a Maxwell-Garnett model based analysis for composites with different types of particle inclusions.[11] It was discovered that the particle size could affect the effective thermal conductivity. Every *et al*. compared the Maxwell-Garnett model and Bruggeman model and discussed the effect of the particle size in the form of a length-unit parameter: Kapitza radius.[12] By combining EMA with their multiple scattering theory, Nan *et al*. developed a model for arbitrary composites where they considered the thermal boundary resistance (TBR) in the form of a coated layer.[13] Duan *et al*. derived an explicit expression for the effective thermal conductivity of heterogeneous media containing ellipsoidal inclusions. More recently, they extended their previous study to include the effect of the imperfect bond between the inclusions and the matrix as well.[14,15]

However, in these models, only phonons are considered, so they are not expected to work well for the metal-matrix composites (MMC) where electrons can make a significant difference.[16] In more recent studies, new methods and modified approaches are developed to take into account these effects. Several works on formulating the two-temperature model (TTM)[17] and Boltzmann transport equations (BTE) have already been presented.[18,19] Combining their previous work with TTM, Miranda *et al*.[20] derived an analysis for the effective thermal conductivity of particulate composites with oriented spheroidal metallic particles embedded in a dielectric matrix. In their following study, extended models which can account for composites in the non-dilute limit were also derived by means of the crowding factor[21] and EMA.[22]

The effect of particle sizes on the effective thermal conductivity has been investigated by several studies,[12,20] but an explicit analytical solution considering electrons' effect has not been given. The critical radius has a significant effect on the effective thermal property; therefore, developing a useful model for predicting r_c is practical for guiding us in choosing the materials and sizes of particles when synchronizing a composite material. Also, modern

a)ruan@purdue.edu

time domain thermal reflectance (TDTR) experiments often involve metal-dielectric multilayers, and it will be beneficial to develop analytical relations that are easy to use. In this study, we combine molecular dynamics (MD) with TTM-Fourier calculations to predict the critical thickness L_c in 1D for metal particles embedded in a polymer matrix. A general solution to TTM that is applicable regardless of the size of the system is derived. The SAM/Au/SAM case study is presented as an example, and TTM-MD simulation is performed to predict the thermal properties for the inputs of the calculation. Based on the mathematical equations and thermal circuit analysis, we propose a new approach to analyze the thermal conduction in metal thin films sandwiched between dielectric layers, which is more intuitive in explaining experimental and simulation results than previous models under certain conditions.[23] Finally, several factors including the thermal conductivity, TBR, and electron-phonon coupling that can affect L_c are discussed.

II. TTM-FOURIER APPROACH

Generally, metals have higher thermal conductivity than polymers. Therefore, when metal particles are added to the polymer matrix, the thermal resistance is expected to be reduced. However, TBR is also introduced at the same time. A 1D representation of this process is illustrated in Fig. 1, where a polymer layer in a polymer block is replaced with metal with the same thickness. The total resistance of the new composite is determined by the competition of the high thermal conductivity of the replaced layer and the introduced TBR. Defining the resistance introduced by the metal middle layer as $R_{intro} = R_{metal,c} + 2R_B$, the net resistance change after the replacement in Fig. 1 can be expressed as

$$\triangle R = R_{intro} - R_{poly,c}. \tag{1}$$

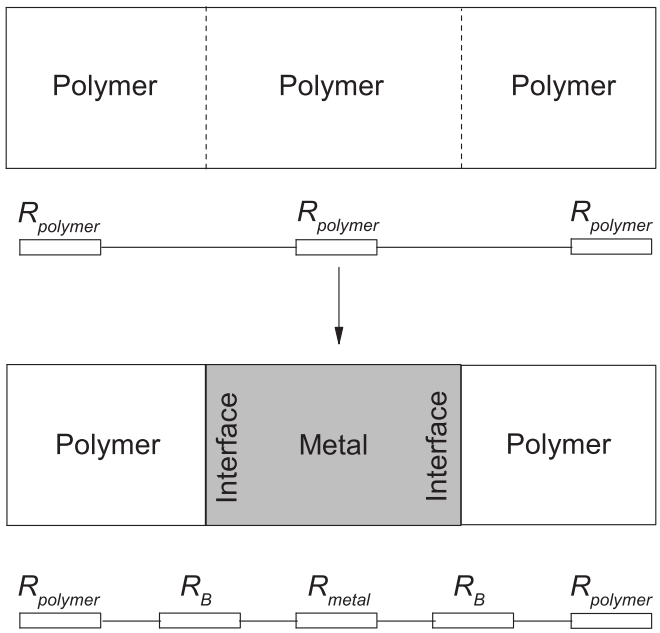

FIG. 1. The schematic of a 1D metal-polymer composite, where a polymer layer is replaced with metal. Hence, the middle layer polymer conduction resistance is replaced by the metal layer conduction resistance and the thermal boundary resistance at the two interfaces.

Here, R_B is the TBR which is related to the material properties such as lattice mismatch, etc. $R_{metal,c}$ and $R_{poly,c}$ refer to the conduction resistance of metal and polymer layers, respectively, which depend on the middle layer thickness and their thermal conductivities. Therefore, $\triangle R$ also varies with these factors. In order to obtain a quantitative analysis of the relationship between $\triangle R$ and the middle layer thickness, expressions for the resistances in Eq. (1) need to be derived.

A. A general solution to two-temperature model equations for a metal thin film sandwiched between two dielectrics

The interfaces in Fig. 1 are the metal/nonmetal interfaces. In metals, thermal transport involves both phonons and electrons. We apply the two-temperature model[17,23] for analysis, where electrons and phonons are depicted as two interacting subsystems with their own temperatures. Their interaction strength is described by the coupling factor G_{ep}. If we ignore all the external factors such as laser heating, etc., the steady-state governing equations are

$$\begin{cases} k_e \dfrac{\partial^2 T_e}{\partial x^2} - G_{ep}(T_e - T_p) = 0, \\ k_p \dfrac{\partial^2 T_p}{\partial x^2} + G_{ep}(T_e - T_p) = 0. \end{cases} \tag{2}$$

Here, T and k denote the temperature and thermal conductivity, respectively, and e and p are the index for electrons and phonons, respectively. In dielectric materials, usually the electrons' effect can be neglected compared with phonons' effect.[23] At the interface, the cross-interface electron-phonon interaction may also be ignored if the temperature difference is not large (<1000 K).[24] Based on the above assumptions, only phonons can transfer energy across the interface, while electrons cannot. In a polymer/metal/polymer sandwich system as illustrated in Fig. 2, the boundary conditions are

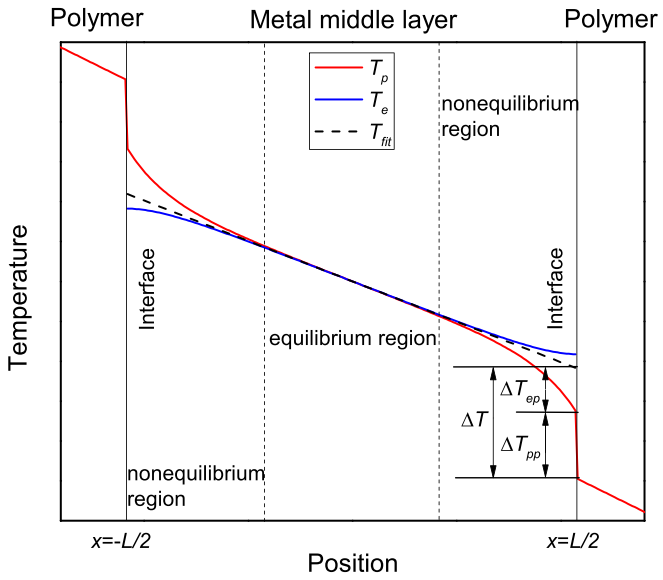

FIG. 2. Temperature distribution in a polymer/metal/polymer sandwich system. In the metal middle layer, both electrons and phonons are considered, while in the polymer substrates only phonons are considered.

$$\begin{cases} -k_{poly}\dfrac{\partial T_{poly}}{\partial x}\Big|_{x=-\frac{L}{2}^-} = -k_p\dfrac{\partial T_p}{\partial x}\Big|_{x=-\frac{L}{2}^+} = J, \\ -k_{poly}\dfrac{\partial T_{poly}}{\partial x}\Big|_{x=\frac{L}{2}^+} = -k_p\dfrac{\partial T_p}{\partial x}\Big|_{x=\frac{L}{2}^-} = J, \\ -k_e\dfrac{\partial T_e}{\partial x}\Big|_{x=-\frac{L}{2}^+} = -k_e\dfrac{\partial T_e}{\partial x}\Big|_{x=\frac{L}{2}^-} = 0, \end{cases} \tag{3}$$

where J is the heat flux and k_{poly} is the thermal conductivity of the polymer. Different boundary conditions cause non-equilibrium between the two energy carriers in the metal. As illustrated in Fig. 2, electrons and phonons have strong non-equilibrium near the interface where their temperatures deviate from each other. This will render an extra interfacial resistance in addition to the phonon-phonon coupling resistance. As a result, the total TBR consists of two parts: $R_B = R_{pp} + R_{ep}$.

R_{pp} can be acquired by several approaches such as the acoustic mismatch model (AMM), diffuse mismatch model (DMM), and MD simulations.[25–27] It can be treated as a relatively constant value at a specific temperature. Therefore, only R_{ep} needs to be derived. Combining Eqs. (2) and (3), we can obtain an expression for the temperature profile in the metal

$$\begin{cases} T_e = T_{mid} - \dfrac{J}{k_p+k_e}x + \dfrac{k_p}{k_p+k_e}\dfrac{Jd}{k_p}\dfrac{\sinh\left(\frac{L}{2d}\right)}{\sinh\left(\frac{L}{d}\right)}\cdot 2\sinh\left(\frac{x}{d}\right), \\ T_p = T_{mid} - \dfrac{J}{k_p+k_e}x - \dfrac{k_e}{k_p+k_e}\dfrac{Jd}{k_p}\dfrac{\sinh\left(\frac{L}{2d}\right)}{\sinh\left(\frac{L}{d}\right)}\cdot 2\sinh\left(\frac{x}{d}\right), \end{cases} \tag{4}$$

where

$$d = \frac{1}{\sqrt{G_{ep}\left(\frac{1}{k_e}+\frac{1}{k_p}\right)}}, \tag{5}$$

is the electron-phonon coupling length. And T_{mid} is the temperature at $x=0$, which is also the center point of the metal middle layer where electrons and phonons reach thermal equilibrium. The total resistance from $x=0$ to $x=\frac{L}{2}^+$ can then be expressed as

$$\frac{T_{mid}-T_R}{J} = \frac{\frac{L}{2}}{k_e+k_p} + \frac{T_p|_{x=\frac{L}{2}^-} - T_{poly}|_{x=\frac{L}{2}^+}}{J} + \frac{k_e}{k_p+k_e}\frac{d}{k_p}\tanh\left(\frac{L}{2d}\right). \tag{6}$$

Here, T_R is the temperature of the polymer at $x=\frac{L}{2}$. Equation (6) has the form of a serial thermal circuit. Observing the right side of Eq. (6), the first term is the definition of the metal conduction resistance from $x=0$ to $x=\frac{L}{2}$, while the second and third term together is the TBR $R_B = R_{pp} + R_{ep}$. By noticing the fact that the second term is exactly the definition of $R_{pp} = \triangle T_p/J$, we can obtain an expression for R_{ep}

$$R_{ep} = \frac{1}{(G_{ep}k_p)^{\frac{1}{2}}}\left(\frac{k_e}{k_e+k_p}\right)^{\frac{3}{2}}\tanh\left(\frac{L}{2d}\right). \tag{7}$$

Equation (7) is generally applicable regardless of the metal film thickness. If we apply the infinite large-system limit, R_{ep} recovers the expression in Wang's work.[23]

B. The critical thickness L_c

With expressions for all the resistances in Eq. (1), $\triangle R$ can be expressed as

$$\triangle R = \frac{2}{(G_{ep}k_p)^{\frac{1}{2}}}\left(\frac{k_e}{k_e+k_p}\right)^{\frac{3}{2}}\tanh\left(\frac{L}{2d}\right) + \frac{2}{h_{pp}} + \frac{L}{k_e+k_p} - \frac{L}{k_{poly}}, \tag{8}$$

where h_{pp} is the phonon thermal boundary conductance (TBC) which is the inverse of R_{pp}.

If we want to improve the heat conduction in the new composite material, $\triangle R$ must be negative so that the total resistance decreases. Observing the first-order derivative of $\triangle R$, it can be shown that

$$\frac{d\triangle R}{dL} < \frac{2}{(G_{ep}k_p)^{\frac{1}{2}}}\left(\frac{k_e}{k_e+k_p}\right)^{\frac{3}{2}} + \frac{1}{k_e+k_p} - \frac{1}{k_{poly}}. \tag{9}$$

For most metals, the value of $k_e + k_p$ is usually greater than 100 W/m K, and G_{ep} is on the order of 1×10^{16} W/m^3 K, while k_{poly} for most common polymer materials is smaller than 10 W/m K. As a result, the right side of Eq. (9) is always negative, which means that $\triangle R$ decreases monotonically as L increases, from its maximum value of $2/h_{pp}$ at $L=0$. The critical thickness L_c is defined as the value where $\triangle R$ crosses zero, and L has to be larger than L_c to result in a negative $\triangle R$. Therefore

$$\frac{2}{(G_{ep}k_p)^{\frac{1}{2}}}\left(\frac{k_e}{k_e+k_p}\right)^{\frac{3}{2}}\tanh\left(\frac{L_c}{2d}\right) + \frac{2}{h_{pp}} + \frac{L_c}{k_e+k_p} - \frac{L_c}{k_{poly}} = 0. \tag{10}$$

It is noteworthy that L_c only exists when $k_{poly} < k_e + k_p$, which is true for most materials. The first term in Eq. (10) makes it difficult to get an explicit analytical solution for L_c. However, we can simplify the equation by taking two extreme limits:

(1) If G_{ep} is very small, which is the case where electrons and phonons have very weak coupling

$$d = \frac{1}{\sqrt{G_{ep}\left(\frac{1}{k_e}+\frac{1}{k_p}\right)}} \to \infty, \frac{L_c}{2d} \to 0, \quad \tanh\left(\frac{L_c}{2d}\right) \to \frac{L_c}{2d}. \tag{11}$$

The first term in Eq. (10) evolves as

$$\frac{2}{(G_{ep}k_p)^{\frac{1}{2}}}\left(\frac{k_e}{k_e+k_p}\right)^{\frac{3}{2}}\tanh\left(\frac{L_c}{2d}\right)=2d\frac{k_e}{k_p(k_e+k_p)}\frac{L_c}{2d}=\frac{k_eL_c}{k_p(k_e+k_p)}. \quad (12)$$

From Eqs. (10) and (12), L_c is expressed as

$$L_c=\frac{\frac{2}{h_{pp}}}{\frac{1}{k_{poly}}-\frac{1}{k_p}}. \quad (13)$$

It is the same result when electrons are not involved. In fact, if $L_c/d<1$, which is usually the case for metals with weak electron-phonon coupling like gold ($L_c/d=0.5$), the above expression is still approximately valid, with an error within 10%.

(2) If G_{ep} is very large, which is the case that electrons and phonons have very strong coupling

$$d=\frac{1}{\sqrt{G_{ep}\left(\frac{1}{k_e}+\frac{1}{k_p}\right)}}\to 0,\frac{L_c}{2d}\to\infty,\quad \tanh\left(\frac{L_c}{2d}\right)\to 1. \quad (14)$$

The first term in Eq. (10) evolves as

$$\frac{2}{(G_{ep}k_p)^{\frac{1}{2}}}\left(\frac{k_e}{k_e+k_p}\right)^{\frac{3}{2}}\tanh\left(\frac{L_c}{2d}\right)=2d\frac{k_e}{k_p(k_e+k_p)}=0. \quad (15)$$

Then

$$L_c=\frac{\frac{2}{h_{pp}}}{\frac{1}{k_{poly}}-\frac{1}{k_p}\frac{1}{1+r_{ep}}},r_{ep}=\frac{k_e}{k_p}. \quad (16)$$

This is the case when electrons and phonons are in perfect equilibrium, indicating that electrons fully contribute to thermal transport. In fact, if $L_c/d>3$, which is usually the case for metals with strong electron-phonon coupling like nickel ($L_c/d=4.1$), the above expression is still approximately valid, with an error of 10%.

(3) When L_c/d is between 1 and 3, the above two simplifications can no longer give accurate results, and we will need to numerically solve Eq. (10) to get an accurate solution. For a specific pair of materials, one can choose one from the above equations with h_{pp}, k_p, and k_{poly} to estimate L_c first, and then check if L_c/d falls in the corresponding range. If so then the approximation is valid, otherwise a more accurate calculation is required.

III. SAM/Au/SAM CASE STUDY

In this section, we will present a case study of a gold thin film sandwiched between aligned SAM chains. The Au/SAM interface has been investigated by several recent studies which could provide benchmarks for our calculations.[28–30] A TTM-MD simulation is performed first to predict the necessary thermal properties, and then, a TTM-Fourier calculation is presented based on the equations introduced in Sec. II.

A. TTM-MD simulation

The TTM-Fourier calculation requires the following thermal properties as known inputs: the phonon TBC h_{pp}, the thermal conductivity k, and the electron-phonon coupling factor G_{ep}. A TTM-MD simulation of a Au/SAM/Au/SAM/Au multilayer system is performed to predict these values.[23,31] The total length of the simulation domain is 134.25 Å, with a cross-section area of 17.304 × 20.0 Å^2 or 12 gold atoms in the (111) plane of the face-centered cubic (FCC) unit cell. 16 SAM molecules form the junction between each 2 adjacent gold layers. As a result, there are 2624 atoms in the domain. Reference of the structure and interatomic potentials used can be found in Refs. 28–30. The electronic properties of gold are taken as the common values at room temperature. The system is first relaxed under zero external pressure condition at 300 K for 0.3 ns, and then, a heat flow of 3.2×10^{-8} W is imposed in the direction which is perpendicular to the interfaces. The nonequilibrium MD simulation runs for another 0.6 ns to let the system get to a steady state. The final temperature profile zoomed at the middle gold layer is shown in Fig. 3. From the results, h_{pp} is 349.3 ± 40.3 MW/m^2 K. Although our h_{pp} agrees reasonably well with previous theoretical predictions,[30] they are significantly higher than reported experimental data such as those reported in Refs. 32 and 33. This is probably because, for example, in simulations the hydrogen atoms are incorporated into their carbon or sulfur backbones and are not simulated explicitly; also the interfaces in simulations are perfectly bonded. Here, we present our results using the theoretical h_{pp}, while the impact of lower h_{pp} (or higher R_{pp}) from experiments on L_c is discussed in Sec. IV B. The lattice thermal conductivity of Au is found to be 6.41 W/m K, while that of the SAM molecule chain ranges from 0.9 W/m K to 2.4 W/m K, which also agree with previous literature studies.[34,35] It is noteworthy that this value is a little bit higher than that of a common polymer matrix. The reason is that these SAM

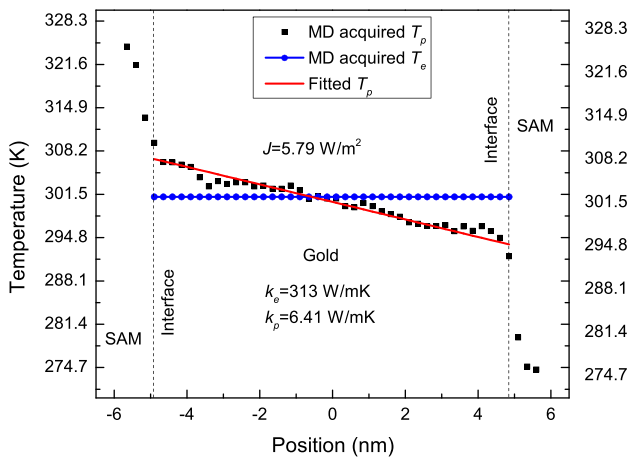

FIG. 3. The temperature profile of the Au/SAM/Au/SAM/Au multiplayer system zoomed at the middle layer from the TTM-MD simulation.

TABLE I. Thermal properties used in TTM-Fourier calculation.

Thermal property	Value
h_{pp}	350 MW/m^2 K
$k_{polymer}$	1.48 W/m K
k_e	313 W/m K
k_p	6.41 W/m K
G_{ep}	2.8×10^{16} W/m^3 K

molecule chains in the system are well aligned. The neat structure ensures that the phonon propagation is smooth and results in a reasonably high thermal conductivity.

B. TTM-Fourier calculations

We have developed equations for estimating L_c in Sec. II. However, usually a more accurate result without approximations is desired. Then, we need to go back to Eq. (10) and acquire the solution through numerical methods. The detailed parameters used for the Au/SAM/Au calculation are listed in Table I. Based on the TTM-MD simulation results, we assign h_{pp} as 350 W/m^2 K for convenience. For the thermal conductivity of polymer, we use our own averaged value of 1.48 W/m K, which is reasonable compared with Chen's result of 2.081 W/m K.[35] $k_e = 313$ W/m K is the bulk electronic thermal conductivity of gold. $G_{ep} = 2.8 \times 10^{16}$ W/m^3 K is a commonly used value for gold.[36] The trend of $\triangle R$ vs. metal film thickness is illustrated in Fig. 4. $\triangle R$ decreases monotonically with the film thickness. And when $\triangle R = 0$, which means that the systems resistance is unchanged, we obtain the critical thickness $L_c = 10.8$ nm. By comparing with the result $L_c = 10.96$ nm given by Eq. (13), we can see that Eq. (13) provides an excellent approximation for metals with weak electron-phonon coupling like gold.

The TTM-Fourier method's prediction of the temperature profile of the entire system is illustrated in Fig. 5. The metal film thickness is chosen as the critical thickness for the SAM/Au/SAM system. The electrons and phonons are

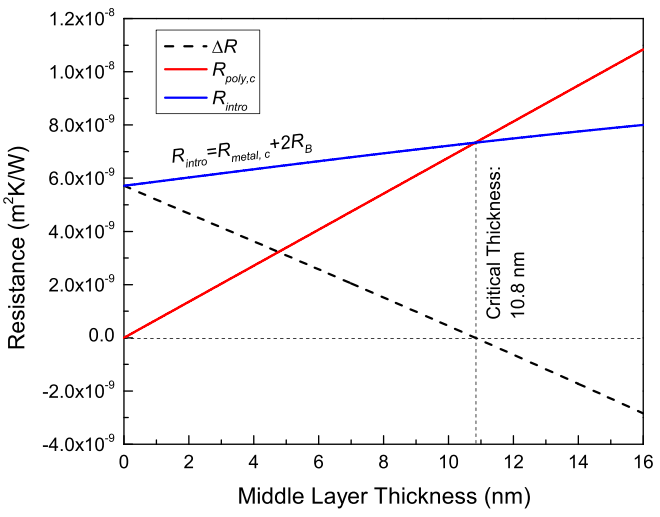

FIG. 4. R_{intro}, $R_{poly,c}$ and $\triangle R$ as a function of the metal layer thickness in the SAM/Au/SAM sandwich system predicted by TTM-Fourier calculation.

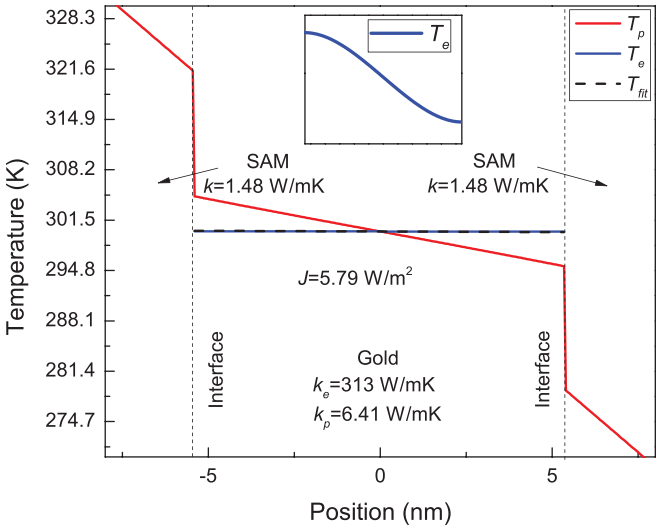

FIG. 5. Temperature profile of a SAM/Au (10.8 nm)/SAM sandwich system predicted by TTM-Fourier calculation. A zoom-in profile of the electron temperature is shown.

in nonequilibrium except at the middle point. Therefore, it justifies the necessity to use our more general Eq. (7) for R_{ep}. The fitted temperature is almost identical to electrons' temperature, which has a very flat profile, indicating a small electronic contribution to the overall thermal conduction. This agrees with Li's result which shows that in very thin metal films phonons dominate the energy transport process.[37]

A closer observation of R_{intro} vs. L also reveals the fact that electrons hardly contribute to the thermal conduction in a thin gold film. As illustrated in Fig. 6, at a thickness smaller than 20 nm R_{intro} mainly comes from R_{pp}, while its increasing trend is mainly determined by R_{ep}'s increase with L. The gradient of R_{intro} is very close to $1/k_p$. This indicates that the R_{intro} curve is almost identical to the straight line with the expression of $R(L) = 2R_{pp} + L/k_p$, which means that the effective thermal transport process is the same as if there is

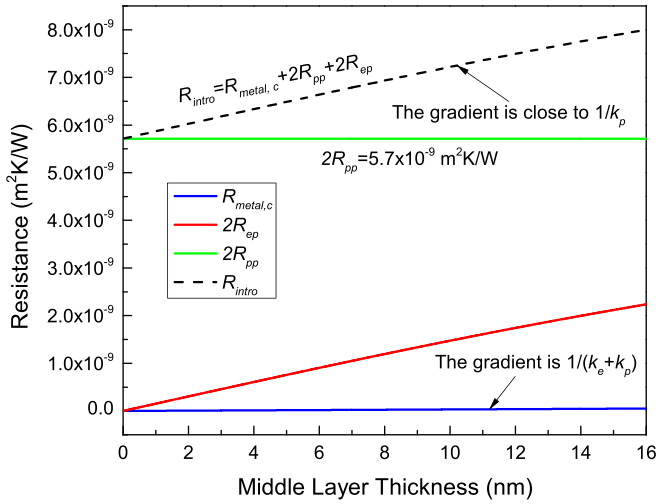

FIG. 6. Components of the total resistance of the gold film. It is composed of three parts: (1) film conduction resistance $R_{metal,c}$, (2) resistance due to interfacial phonon coupling R_{pp}, (3) resistance due to electron-phonon nonequilibrium near the interface R_{ep}. It is revealed that $R_{metal,c}$ comprises a very small part. The majority of the resistance comes from R_{pp} and R_{ep}.

only phonon participation. This stimulates our proposal for a new analytical approach for thermal conduction in sandwiched metal thin films, which will be discussed in Sec. IV A.

IV. DISCUSSION

A. The effective thermal conductivity of the sandwiched metal layer

So far, we have assumed that the thermal conductivity of the metal layer is still $k_e + k_p$, while we lump R_{ep} into the interface resistance. This is commonly done for a single interface between semi-infinite metal and dielectric,[17,23] since electrons and phonons are in equilibrium in nearly the entire metal except for the short cooling region near the interface. However, it is not so intuitive for the sandwiched thin film here since electrons and phonons are in strong non-equilibrium except for the mid-plane, and the thermal conduction is dominated by phonons. Therefore, it is more intuitive to start the metal layer as a phonon-only system, and investigate what effects the electrons will bring. Therefore, here we present an alternative analysis where we define a new effective thermal conductivity of the metal layer while not assuming it to be $k_e + k_p$ anymore.

From Eq. (7), we can express R_{intro} as follows:

$$\begin{aligned} R_{intro} &= 2R_{ep} + R_{metal,c} + 2R_{pp} \\ &= \frac{2}{(G_{ep}k_p)^{\frac{1}{2}}}\left(\frac{k_e}{k_e+k_p}\right)^{\frac{3}{2}}\tanh\left(\frac{L}{2d}\right) + \frac{L}{k_e+k_p} + 2R_{pp}. \end{aligned} \tag{17}$$

Previously, we have treated R_{ep} as part of R_B. Here, we view the metal layer primarily as a phonon system, so we only include R_{pp} in R_B, while lumping R_{ep} into the conduction resistance of the metal layer R_{eff}. Therefore,

$$\begin{aligned} R_{eff} &= 2R_{ep} + R_{metal} \\ &= \frac{2}{(G_{ep}k_p)^{\frac{1}{2}}}\left(\frac{k_e}{k_e+k_p}\right)^{\frac{3}{2}}\tanh\left(\frac{L}{2d}\right) + \frac{L}{k_e+k_p}, \end{aligned} \tag{18}$$

and then define the effective thermal conductivity of the metal film as

$$k_{eff} = \frac{L}{R_{eff}} = \frac{k_e+k_p}{1 + \frac{2k_e}{L}\left[\frac{k_e}{G_{ep}k_p(k_e+k_p)}\right]^{\frac{1}{2}}\tanh\left(\frac{L}{2d}\right)}. \tag{19}$$

The corresponding thermal circuit is shown in Fig. 7. And we can easily find that

$$\begin{aligned} &k_{eff} \to k_p, \quad \text{when } L \to 0 \text{ or } G_{ep} \to 0, \\ &k_{eff} \to k_e + k_p, \quad \text{when } L \to \infty \text{ or } G_{ep} \to \infty. \end{aligned} \tag{20}$$

This indicates that: (1) in a sandwiched metal film that is very thin (or has very weak electron-phonon coupling), the effective thermal conductivity is identical to its lattice portion and electrons are as if not involved at all. We call this the "thin limit." And (2) when the metal is thick (or has strong electron-phonon coupling), the effective thermal conductivity recovers the bulk value, and we call it the "thick limit."

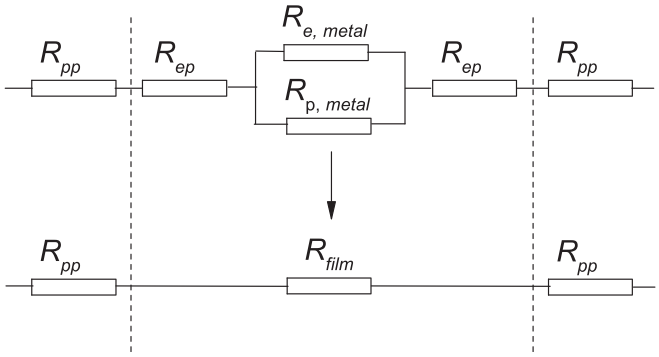

FIG. 7. A new thermal circuit for a sandwiched metal thin film where R_{ep} is lumped into R_{eff}.

We expect that this interpretation, especially the thin limit, to be very useful for experimentalists. In experiments, R_{pp} is often treated as the only TBR.[38] It is then straightforward to match the measured values with components of the thermal circuit in Fig. 7. If the thin limit applies, k_{eff} should become the lattice thermal conductivity while not the bulk metal conductivity $k_e + k_p$, This provides an intuitive way to check and interpret experiments.

A more detailed dependence of k_{eff} on the film thickness is illustrated in Fig. 8. Gold is still taken as the example here. It can be observed that the thin limit is valid when the thickness is much smaller than the electron-phonon cooling length of 45 nm,[23] as k_{eff} remains below $110\%k_p$ when L is below 16.2 nm. In this range, which is usually the case for a metal thin film sandwiched between dielectric materials, our new approach where R_{ep} is included as part of the film conduction resistance is more intuitive. Our model bypasses electrons' effect and only requires lattice temperature measurements for analysis, and the measured effective thermal conductivity k_{eff} is simply k_p. As L increases, k_{eff} starts to deviate from k_p and eventually converges to $k_e + k_p$. For a thickness larger than 10.2 μm, which is more than 200 times larger than the cooling length, k_{eff} can be approximated as $k_e + k_p$ with an error smaller than 10%. In this range, which is usually the case when investigating an interface between two semi-infinite blocks, the original thermal circuit where R_{ep} is part of the TBR works better. The experimentally measured k_{eff} can no longer be interpreted by k_p. When L falls in the transition region marked in Fig. 8, an accurate analysis requires utilization of the exact form of Eq. (18) and investigation of the corresponding serial thermal circuit.

B. Factors affecting L_c

In this section, we discuss several factors that can affect L_c based on Eq. (10): (1) R_{pp}, (2) G_{ep}, (3) k_p, (4) k_{poly}, and (5) r_{ep}.

(1) R_{pp} comprises the most part of TBR when the metal film is as thin as ~10 nm. A larger R_{pp} will increase TBR, thus increasing the critical thickness. For example, if one uses the experimentally determined R_{pp}[32,33] which is much higher than the one we used in our previous

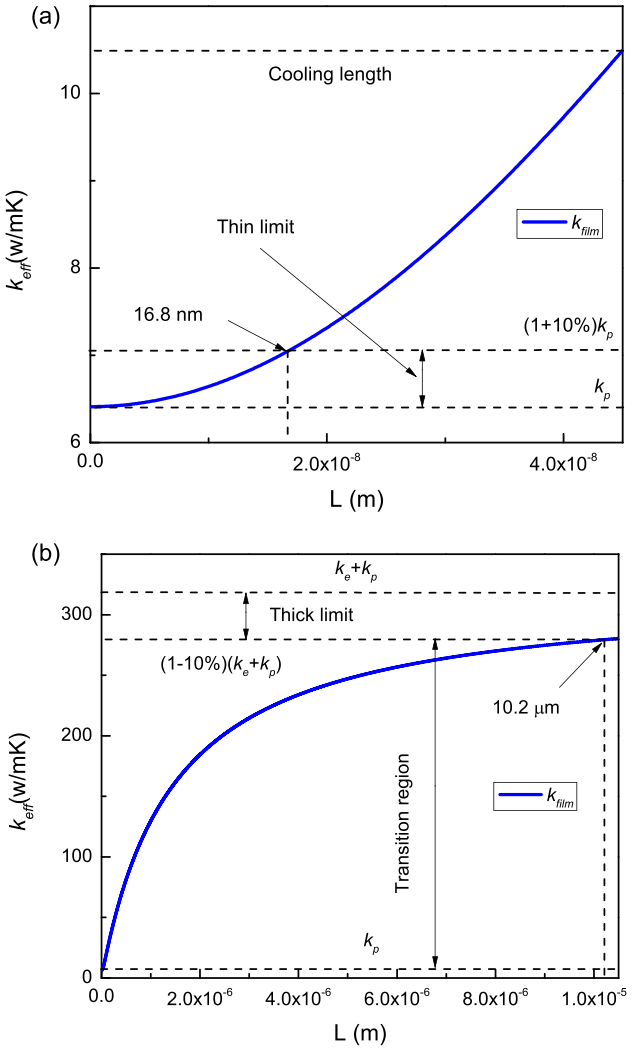

FIG. 8. (a) k_{eff} vs. L for gold when L is within the electron-phonon cooling length, which is 45 nm for gold. (b) k_{eff} vs. L for gold when L over a large range of thickness. k_{eff} eventually converges to its saturated value of $k_e + k_p$.

calculations, the resulting L_c will be larger than 10.8 nm, but the general trend is the same and our conclusions are still valid.

(2) G_{ep} measures the electron-phonon coupling strength and is directly related to R_{ep}. A larger G_{ep} will render a smaller R_{ep} and thus a smaller TBR, resulting in a smaller critical thickness.

(3) k_p dominates the thermal transport process in thin films as mentioned above. As a result, it is almost identical to the effective thermal conductivity k_{eff}. When k_p increases, k_{eff} increases, R_{ep} will decrease according to Eq. (7); hence, the critical thickness will be smaller.

(4) k_{poly} is the thermal conductivity of the polymer matrix. A larger k_{poly} will increase the difficulty for the metal film to compensate for the resistance increase due to introduced TBR after the replacement. Therefore, larger k_{poly} will result in larger L_c.

(5) r_{ep}, which is the ratio of k_e over k_p, can affect R_{ep} as well as the thermal conductivity of the metal film. If we keep k_p as fixed, larger r_{ep} will increase $k_e + k_p$ and also change R_{ep} (whether it will increase or decrease depends). Generally, a larger k_e is beneficial and will result in a smaller L_c. The effect is more significant if the values of k_e and k_p are comparable which means that r_{ep} is around 1, especially for large G_{ep}.

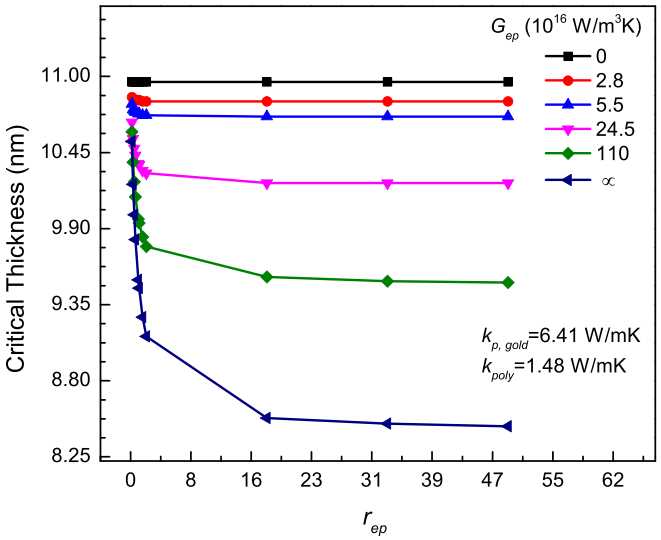

FIG. 9. Two main factors that can affect the critical thickness L_c: G_{ep} and k_e. It is revealed that G_{ep} has a significant effect on L_c. L_c is sensitive to k_e as k_e is small (small r_{ep}), while it becomes insensitive as k_e becomes large.

When we choose the filler material to add into the polymer matrix, two characteristic properties are G_{ep} and k_e. Here, we plot G_{ep} and k_e's effect on L_c in Fig. 9 on an arbitrary SAM/Au/SAM system to gain a more straight-forward insight. k_p is fixed at the value of gold's lattice thermal conductivity, and k_e is represented by the normalized parameter r_{ep}. L_c decreases with larger G_{ep} and larger k_e. However, k_e's effect is only significant when k_e is small and the impact vanishes as k_e increases. However, metals usually have much larger k_e than k_p, so r_{ep} is not so significant in controlling L_c.

V. SUMMARY

We have proposed a TTM-Fourier approach with input parameters from TTM-MD to predict the critical thickness L_c for metal particle-polymer composite in 1D. A general solution to TTM for thermal transport in a metal film sandwiched between dielectric materials is derived. As an example, L_c for the 1D SAM/Au/SAM system is calculated to be around 10.8 nm. Based on the theoretical equations, we define an effective thermal conductivity for sandwiched metal thin films and propose a new thermal circuit analysis that are intuitive to interpret experimental results. A detailed discussion on the applicable range of our model is presented. It is shown that when the metal film is much thinner than its electron-phonon cooling length (thin limit), the effective thermal conductivity reduces to just the phonon part. For a metal layer with a large thickness (thick limit), the conventional thermal circuit is more advantageous, and the effective thermal conductivity recovers the metal bulk value. For the thickness in between the two limits, our general TTM solution still provides an accurate method for analysis. Finally, several factors affecting L_c are discussed, and it is discovered

that the thermal conductivity, TBR, and the electron-phonon coupling factor all play important roles in determining L_c, which can provide us with a general guidance in the choice of materials when synchronizing a new composite.

[1]E. S. Toberer, L. L. Baranowski, and C. Dames, Annu. Rev. Mater. Res. **42**, 179 (2012).
[2]R. Yang and G. Chen, Phys. Rev. B **69**, 195316 (2004).
[3]X. Shen, Z. Wang, Y. Wu, X. Liu, Y.-B. He, and J.-K. Kim, Nano Lett. **16**, 3585 (2016).
[4]K. M. F. Shahil and A. A. Balandin, Nano Lett. **12**, 861 (2012).
[5]M. Law, J. Goldberger, and P. Yang, Annu. Rev. Mater. Res. **34**, 83 (2004).
[6]J. C. Maxwell, *Electricity and Magnetism* (Clarendon Press, Oxford, 1873).
[7]A. N. Norris, P. Sheng, and A. J. Callegari, J. Appl. Phys. **57**, 1990 (1985).
[8]H. Hatta and M. Taya, J. Appl. Phys. **59**, 1851 (1986).
[9]Y. Benveniste, J. Appl. Phys. **61**, 2840 (1987).
[10]Y. Benveniste and T. Miloh, J. Appl. Phys. **69**, 1337 (1991).
[11]D. Hasselman and L. F. Johnson, J. Composite Mater. **21**, 508 (1987).
[12]A. Every, Y. Tzou, D. Hasselman, and R. Raj, Acta Metall. Mater. **40**, 123 (1992).
[13]C.-W. Nan, R. Birringer, D. R. Clarke, and H. Gleiter, J. Appl. Phys. **81**, 6692 (1997).
[14]H. Duan, B. Karihaloo, J. Wang, and X. Yi, Phys. Rev. B **74**, 195328 (2006).
[15]H. Duan and B. Karihaloo, Phys. Rev. B **75**, 064206 (2007).
[16]A. Mortensen and J. Llorca, Annu. Rev. Mater. Res. **40**, 243 (2010).
[17]A. Majumdar and P. Reddy, Appl. Phys. Lett. **84**, 4768 (2004).
[18]B. Yilbas and S. B. Mansoor, Phys. B: Condens. Matter **407**, 4643 (2012).
[19]Y. Wang, Z. Lu, A. K. Roy, and X. Ruan, J. Appl. Phys. **119**, 065103 (2016).
[20]J. Ordonez-Miranda, R. Yang, and J. J. Alvarado-Gil, J. Appl. Phys. **111**, 044319 (2012).
[21]J. Ordonez-Miranda, R. Yang, and J. J. Alvarado-Gil, J. Appl. Phys. **114**, 064306 (2013).
[22]J. Ordonez-Miranda, J. J. Alvarado-Gil, and R. Yang, Int. J. Thermophys. **33**, 2118 (2012).
[23]Y. Wang, X. Ruan, and A. K. Roy, Phys. Rev. B **85**, 205311 (2012).
[24]P. E. Hopkins and P. M. Norris, Appl. Surf. Sci. **253**, 6289 (2007).
[25]E. Swartz and R. Pohl, Rev. Mod. Phys. **61**, 605 (1989).
[26]R. J. Stevens, L. V. Zhigilei, and P. M. Norris, Int. J. Heat Mass Transfer **50**, 3977 (2007).
[27]E. S. Landry and A. J. H. McGaughey, J. Appl. Phys. **107**, 013521 (2010).
[28]J. Aizenberg, A. J. Black, and G. M. Whitesides, J. Am. Chem. Soc. **121**, 4500 (1999).
[29]I.-H. Sung and D.-E. Kim, Appl. Phys. A **81**, 109 (2005).
[30]T. Luo and J. R. Lloyd, Int. J. Heat Mass Transfer **53**, 1 (2010).
[31]Z. Lu, Y. Wang, and X. Ruan, Phys. Rev. B **93**, 064302 (2016).
[32]M. D. Losego, M. E. Grady, N. R. Sottos, D. G. Cahill, and P. V. Braun, Nat. Mater. **11**, 502 (2012).
[33]R. Y. Wang, R. A. Segalman, and A. Majumdar, Appl. Phys. Lett. **89**, 173113 (2006).
[34]D. Segal, A. Nitzan, and P. Hanggi, J. Chem. Phys. **119**, 6840 (2003).
[35]A. Henry and G. Chen, Phys. Rev. Lett. **101**, 235502 (2008).
[36]Z. Lin, L. Zhigilei, and V. Celli, Phys. Rev. B **77**, 075133 (2008).
[37]Z. Li, S. Tan, E. Bozorg-Grayeli, T. Kodama, M. Asheghi, G. Delgado, M. Panzer, A. Pokrovsky, D. Wack, and K. E. Goodson, Nano Lett. **12**, 3121 (2012).
[38]X. Wu, J. Walter, T. Feng, J. Zhu, H. Zheng, J. F. Mitchell, N. Bikup, M. Varela, X. Ruan, C. Leighton, and X. Wang, Adv. Funct. Mater. **27**, 1704233 (2017).